28 Mar 2001, 2:00 pm - 2:45 pm

Deep Foundations in Liquefiable Soils: Case Histories, Centrifuge Tests and Methods of Analysis

W. D. Liam Finn
Kagawa University, Japan

T. Thavaraj
University of British Columbia, Canada

DEEP FOUNDATIONS IN LIQUEFIABLE SOILS: CASE HISTORIES, CENTRIFUGE TESTS AND METHODS OF ANALYSIS

W.D. Liam Finn
Anabuki Chair of Foundation Geodynamics
Kagawa University, Takamatsu, Japan

T. Thavaraj
Research Associate, Civil Engineering Department
University of B.C., Vancouver, B.C., Canada

ABSTRACT

This paper describes the performance of pile foundations in liquefied soils. Two different aspects of pile response are considered, seismic response to earthquake shaking and response to lateral spreading when the liquefied ground is sloping. The case histories show that piles can be designed economically to resist large lateral displacements and that most of the reported examples of damage from lateral spreading involve weak piles with little reinforcement which were installed to control vertical settlements and were not designed to be moment resistant.

A quasi-3-D continuum method is presented for dynamic effective stress response analysis of pile groups in liquefiable soils. The method is validated using data from centrifuge tests. Methods are presented also for the analysis of piles due to lateral spreading.

BEHAVIOUR OF PILE FOUNDATIONS DURING EARTHQUAKES

During strong earthquake shaking, loose cohesionless sands and silts below the water table develop high porewater pressures that lead to losses in strength and stiffness. If the porewater pressure reaches the level of the effective overburden pressure, liquefaction occurs with almost a complete loss of strength and stiffness. If the liquefied layer is near the surface, the high porewater pressure may vent through a nonliquefied surface layer, giving rise to the features called sand boils, shown in Fig. 1. The presence of sand boils is one of the most common indicators of the occurrence of liquefaction. Liquefaction has serious consequences for the performance of pile foundations that must be considered in design.

During liquefaction large ground displacements can take place on sloping ground or towards an open face such as a river bank. Displacements during the 1964 Niigata earthquake are shown in Fig. 2. Some of these displacements were as large as 10m. Such displacements have been very damaging to pile foundations. Damage to a pile in Niigata caused by 2m of ground displacement is shown in Fig. 3. The complete shearing of a pile in Port Island by about 2m of ground displacement during the 1995 Kobe earthquake is shown in Fig. 4. These piles were designed for vertical loads only, and could not carry the large moments and shears induced by ground displacements and earthquake shaking.

Fig. 1. Sand boils indicating ground liquefaction.

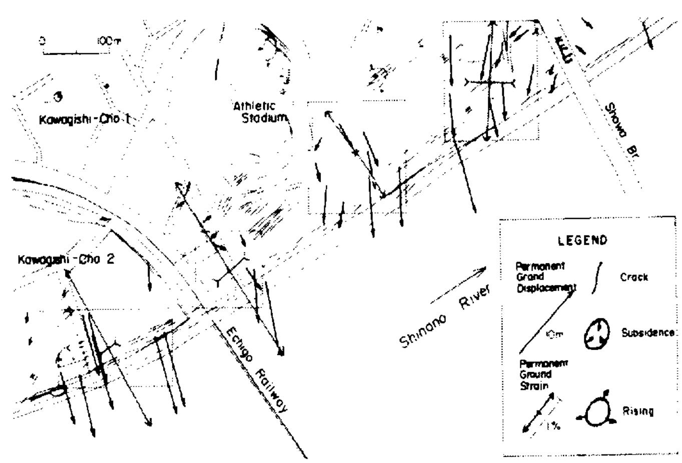

Fig. 2. Ground displacements in Niigata during the 1964 earthquake.

Fig. 3. Damage to pile by ground displacement, Niigata 1964.

Fig. 4. Shearing of a pile by ground displacement in Kobe earthquake, 1995.

However piles can be designed to carry the moments and shears generated by earthquake shaking or post-liquefaction large ground displacements. Some examples of successful design are now presented. Figure 5 shows a bridge on pile foundations at Hachirogata, near Akita. The foundation soils liquefied during the 1983 Nihon-Kai-Chubu earthquake. This led to a failure of the approach embankments by lateral spreading but the pile foundations survived without damage. During the 1995 Kobe earthquake, the ground around the ferry building on Port Island moved about 2.5m towards the sea and settled about 1.8m as shown in Fig. 6. Despite these large displacements, the piles supporting the ferry building showed no damage (Fig. 7). Figure 8 shows a pile supporting a crane rail on Port Island. The ground has moved almost 1.0m but the pile is undamaged. This pile was designed to carry the lateral loads from crane operations and consequently had considerable moment resistance.

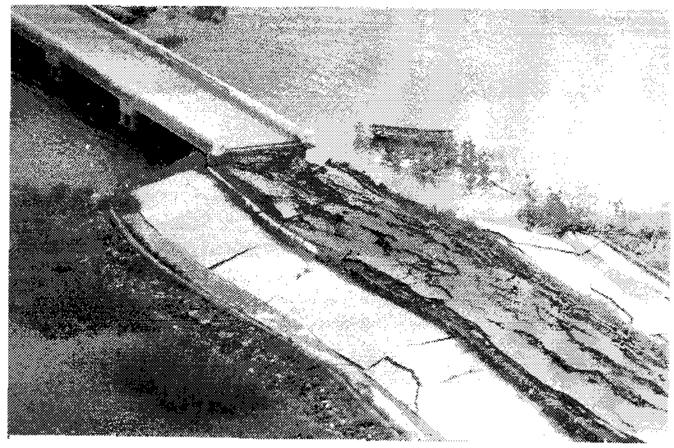

Fig. 5. Bridge on undamaged pile foundations with failed embankment; Nihon-kai-chubu earthquake, 1983.

Fig. 6. Large ground displacements around the ferry building on Port Island after the Kobe earthquake, 1995.

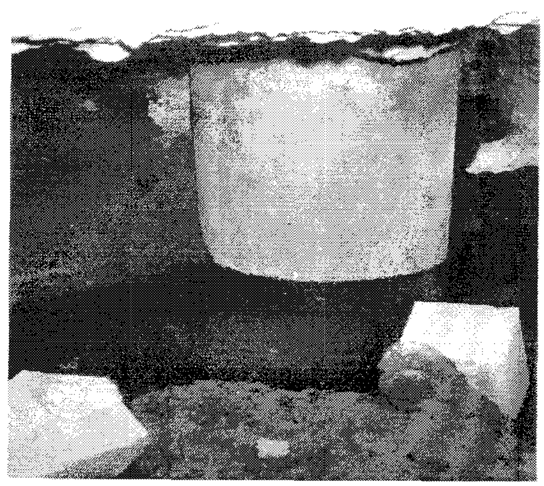

Fig. 7. Undamaged pile under ferry building in Port Island after Kobe earthquake, 1995.

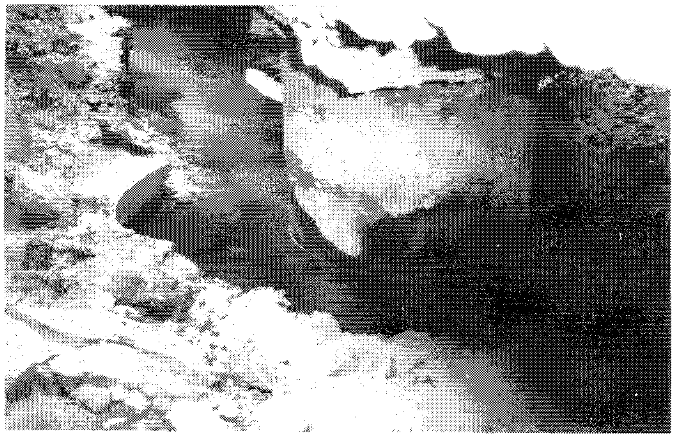

Fig. 8 Undamaged pile supporting a crane rail in ground which moved more than 1.0m.

A typical consequence of widespread liquefaction around pile foundations of bridges is the collapse of sections of the bridge deck because of large relative displacements occurring between the piers. One of the more dramatic examples of this is the failure of the newly constructed Showa Bridge in Niigata during the 1964 Niigata earthquake (Fig. 9).

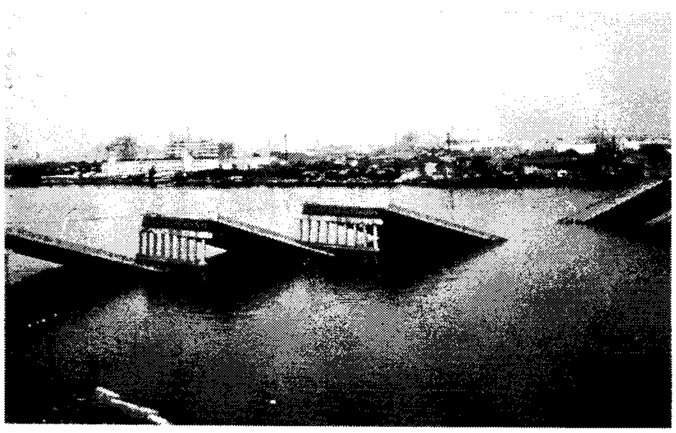

Fig.9. Collapse of the Showa bridge during the Niigata earthquake in 1964.

This type of failure has been seen in a number of earthquakes since then, most recently during the 1995 Kobe earthquake, when a segment of the deck of the Nishinomiya Bridge carrying the Harbour Freeway around Osaka Bay, between Osaka and Rokko Island, collapsed (Fig. 10). This is a very interesting case history and therefore it is discussed is some detail in the next section.

NISHINOMIYA BRIDGE

The Nishinomiya bridge links two reclaimed islands, Nishinomiya and Koshien, along the bay shore freeway between Osaka and Rokko Island. Longitudinal sections of the bridge and foundation soils are shown in Fig. 11. The bridge is supported on Piers P 99 and P 100. The soil in the

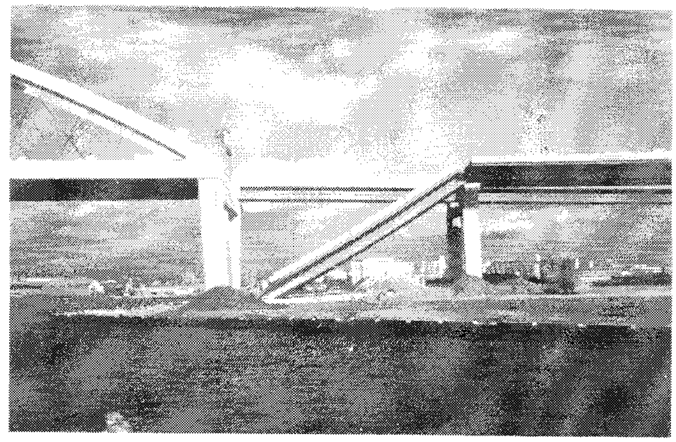

Fig.10. Collapse of the deck of Nishinomiyako bridge during the Kobe earthquake

top 6m-8m is loose reclaimed sand, with standard penetration test, N, values of 10 or less, overlying alluvial soft clay (Ac1). The bridge foundations rest on dense sand (As1) and diluvial gravels, clays and sands underly the alluvial clay. The caisson foundation for pier P 100 is 42m x 22m in plan and 23m high, that for pier P 99 is 40m x 13m in plan and 23m high. During the 1995 Kobe earthquake, the steel girders spanning between P 99 and P 98 fell off Pier P 99 (Fig. 10). The seating length at P 99 was 110cm.This meant that the relative displacement between the top of the pier and the girders was during the earthquake was at least 110 cm.

The reclaimed land on both sides of the bridge liquefied and lateral spreading occurred towards the channel with a magnitude of 1m-2m at the quay walls. Initially the liquefaction and large ground displacements were considered the likely causes of failure. However post-earthquake investigations showed that the caissons moved only slightly towards the channel; 1cm-5cm on the Nishinomiya side and 1cm-9cm on the Koshien side. At the top of Pier P 99 the residual horizontal displacement was only 17cm, much less than the required displacements of 110cm. Clearly lateral spreading was not the primary cause of failure.

A complete dynamic analysis of the bridge and foundations was conducted by investigators to determine the source of the large deformations. The bridge was modeled as a linear framed structure. The foundation soils were assumed elastic but the degradation of shear modulus with shear strain was taken into account. The dynamic analysis showed a potential displacement of 87cm: 8cm from translation of the caisson, 26cm from rotation of the caisson and 57cm from bending of the bridge pier. Clearly pier flexibility contributed the most to the damaging displacements. Direct translations of the piers contributed very little. How the superstructure responds to the seismic displacements, however, depends on the capacity of the connections and restrainers at the top of the pier. In this case the restrainers failed.

Repairs to the bridge were based on these findings. No remedial treatment was carried out on the foundations but

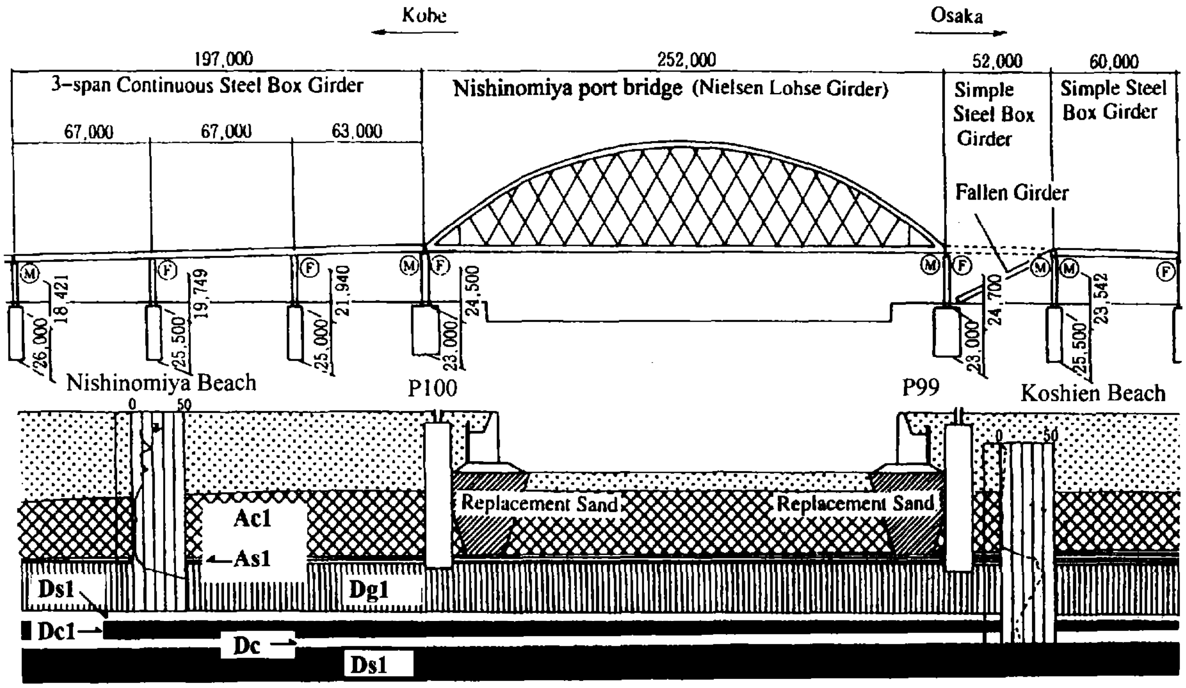

Fig. 11. Cross-section of Nishinomiya Bridge and foundation soil.

connectors with higher ultimate strengths were installed on the piers. Compaction grouting was carried out near the quay walls to reduce wall displacements in future earthquakes.

This case history shows the importance of a detailed dynamic analysis in tracking down the reasons for failures during earthquakes. Such analyses are equally important in evaluating final designs of important structures.

DISPLACEMENT ANALYSIS

In the case histories section, it was shown that large post liquefaction displacements can occur and that these can be very damaging to pile foundations. The deformed shape of a pile foundation caused by these post-liquefaction displacements is illustrated in Fig. 12. These potential deformations often control design in weak highly liquefiable soils. It is very difficult to predict these displacements reliably. In engineering practice, the displacements at the top of the liquefied layer are estimated by empirical formulas based on field data from past earthquakes. The first predictor equation was developed by Hamada et al. [1986] in Japan. Very comprehensive predictor equations have been developed by Youd [1993] which are widely used in practice in North America. A very simple relation is given by the Japan Water Works Association Code [JWWA, 1997] based only on ground slope and the thickness of the liquefied layer.

The estimated lateral displacements are assumed to vary linearly or as a cosine curve from top to bottom of the liquefied layer. These displacements are applied to the springs of the near field portion of the general Winkler model in Fig. 13. Displacements, bending moments and shears are

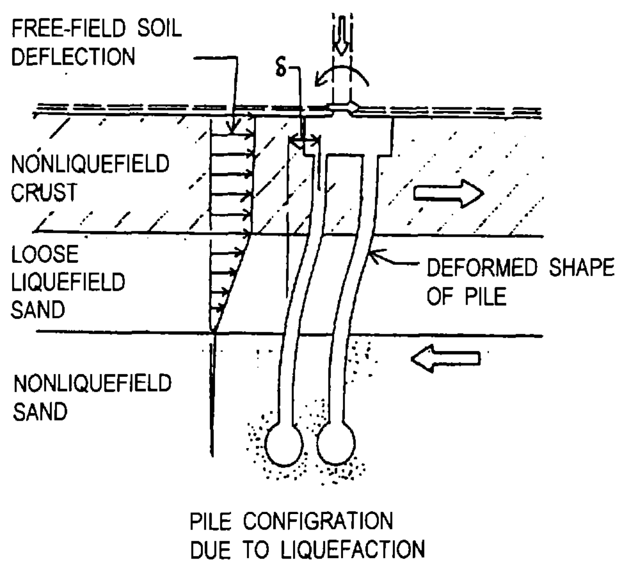

Fig.12. Distortion of pile foundation by moving soil.

calculated using static analysis (dushpots not used).

A force based analysis is recommended by JWWA [1997]. An unliquefied layer as in Fig. 12 is assumed to apply passive pressure to the pile. A liquefied layer is assumed to apply a pressure not more than 30% of the total overburden pressure.

SEISMIC RESPONSE ANALYSIS

The most common approach to the analysis of pile foundations is to use Winkler springs and dashpots to simulate soil stiffness and damping. The springs may be elastic or nonlinear. Some organizations such as the American Petroleum Institute [API, 1993] gives specific guidance for the development of nonlinear load-deflection (p-y) curves as a function of soil properties that can be used to represent nonlinear springs. The API (p-y) curves, which are the most widely used in engineering practice, are based on data from static and slow cyclic loading tests in the field.

The most general Winkler model is shown in Fig. 13. The near field interaction between pile and soil is modeled by springs and dashpots. The near field pile-soil system, together with any structural mass included with the pile, are excited by the seismic base motions and the free field motions applied to the end of each Winkler spring. The free field motions at the desired elevations in the soil layer are computed by 1-D dynamic analyses using a program such as SHAKE [Schnabel et al. 1972].

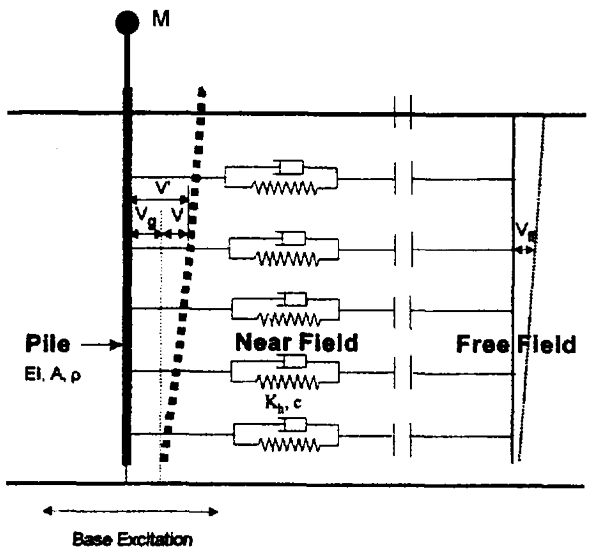

Fig. 13. A Winkler spring model for pile analysis.

An alternative to the Winkler type computational model is to use a finite element continuum analysis based on the actual soil properties. Dynamic nonlinear finite element analysis in the time domain using the full 3-dimensional wave equations is not feasible for engineering practice at present because of the time needed for the computations. However, by relaxing some of the boundary conditions associated with a full 3-D analysis, it is possible to get reliable solutions for nonlinear response of pile foundations with greatly reduced computational effort. The results are very accurate for excitation due to horizontally polarized shear waves propagating vertically [Wu, 1994; Finn and Wu, 1994]. A full description of this method, including numerous validation studies, has been presented by Wu and Finn [1997a,b]. The method is incorporated in the computer program PILE-3D.

The (p-y) curves used in the Winkler computational models are based on static and slow cyclic loading tests. The reliability of these (p-y) curves for the analysis of pile foundations even under static and slow cyclic loading has been shown to be relatively low [O'Neill and Murchison, 1983, Murchison and O'Neill, 1984]. There is very little quantitative data on the seismic response of pile foundations and much of that is not readily accessible. In recent years, seismic loading of model pile foundations in centrifuge tests has provided data that allows a more realistic evaluation of the reliability of various methods for the seismic analysis of pile foundations. Results of API-Winkler and PILE-3D analyses of pile response to strong and low level shaking are compared with test data in Figs 14 and 15. The Winkler analysis over predicts the peak moment from shaking by about 50% in the strong shaking case but gives very good results for low levels of shakings. Details of and comments on these analyses may be found in Finn et al [1999].

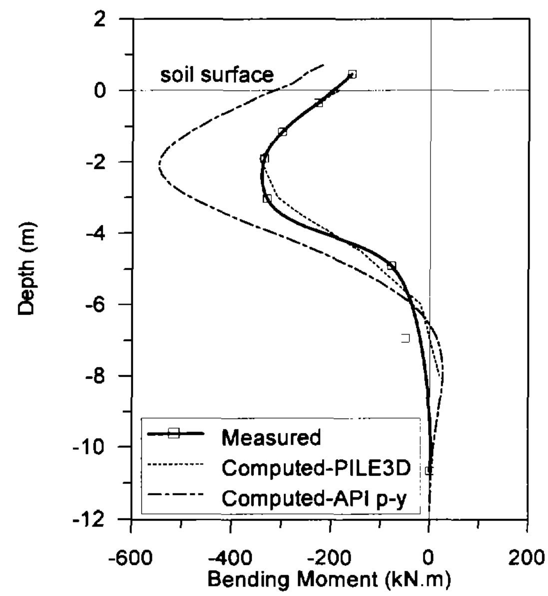

Fig. 14. Comparison of measured and computed bending moments.

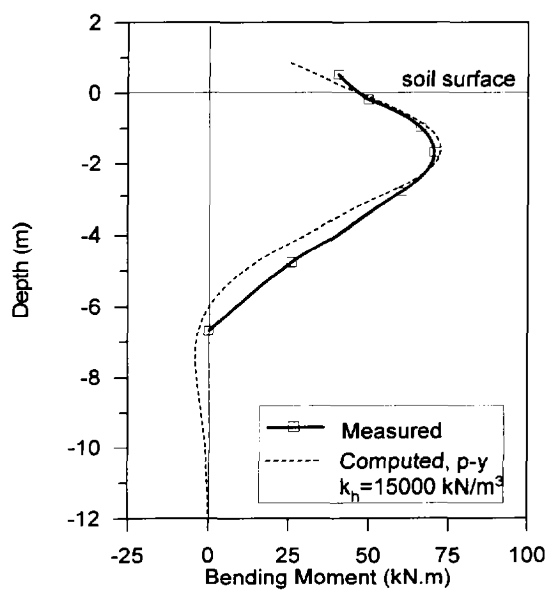

Fig. 15. Comparison of measured and computed pile moments for near elastic response using API procedure.

OUTLINE OF PILE-3D ANALYSIS

A brief outline is given of the basis of the PILE-3D analysis. For details, the reader is referred to Wu and Finn [1997a,b]. The basic assumptions of the simplified 3D analysis are illustrated in Fig. 16. Under vertically propagating shear waves the soil undergoes primarily shearing deformations in xOy plane except in the area near the pile where extensive compressional deformations develop in the direction of shaking. The compressional deformations also generate shearing deformations in yOz plane. Therefore, the assumptions are made that dynamic response is governed by the shear waves in the xOy and yOz planes and compressional waves in the direction of shaking, Y. Deformations in the vertical direction and normal to the direction of shaking are neglected. Comparisons with full 3D elastic solutions confirm that these deformations are relatively unimportant for horizontal shaking. Applying dynamic equilibrium in the Y-direction, the dynamic governing equation of the soil continuum in free vibration is written as

$$\rho_s \frac{\partial^2 v}{\partial t^2} = G^* \frac{\partial^2 v}{\partial x^2} + \theta G^* \frac{\partial^2 v}{\partial y^2} + G^* \frac{\partial^2 v}{\partial z^2} \qquad (1)$$

where G^* is the complex modulus, v is the displacement in the direction of shaking, ρ_s is the mass density of soil, and θ is a coefficient related to Poisson's ratio of the soil. Piles are modeled using ordinary Eulerian beam theory. Bending of the piles occurs only in the yOz plane. Dynamic soil-pile-structure interaction is maintained by enforcing displacement compatibility between the pile and soils.

A finite element code PILE-3D was developed to incorporate the dynamic soil-pile-structure interaction theory described above. An 8-node brick element is used to represent soil

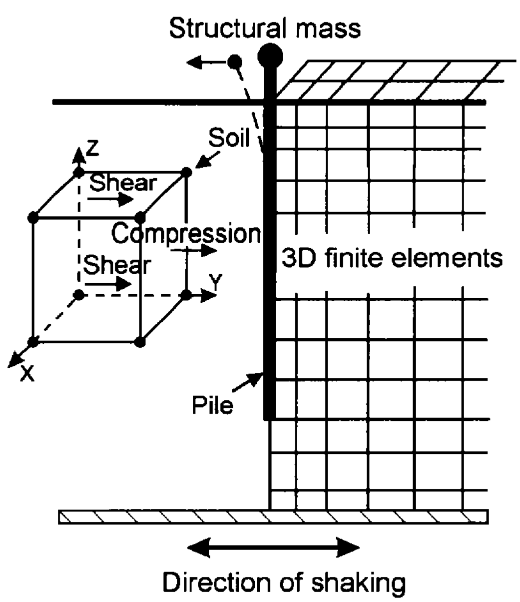

Fig. 16. Quasi-3D model of pile-soil response.

and a 2-node beam element is used to simulate the piles, as shown in Fig. 16. The global dynamic equilibrium equation in matrix form is written as

$$[M]\{\ddot{v}\} + [C]\{\dot{v}\} + [K]\{v\} = -[M]\{I\} \cdot \ddot{v}_0(t) \qquad (2)$$

in which $\ddot{v}_0(t)$ is the base acceleration, {I} is a unit column vector, and $\{\ddot{v}\},\{\dot{v}\}$ and {v} are the relative nodal acceleration, velocity and displacement, respectively.

The loss of energy due to radiation damping is modeled using the method proposed by Gazetas et al. [1993] for elastic response in which a velocity proportional damping force F_d per unit length is applied along the pile. Direct step-by-step integration using the Wilson-θ method is employed in PILE-3D to solve the equations of motion in Equation (2). The nonlinear hysteretic behaviour of soil is modeled by using an equivalent linear method in which properties are varied continuously as a function of soil. Typical shear strain dependencies of the shear modulus and damping ratio of sand, shown in Fig. 17, were proposed by Seed and Idriss [1970]. Additional features such as tension cut-off and shearing failure are incorporated in the program to simulate the possible gapping between soil and pile near the soil surface and yielding in the near field.

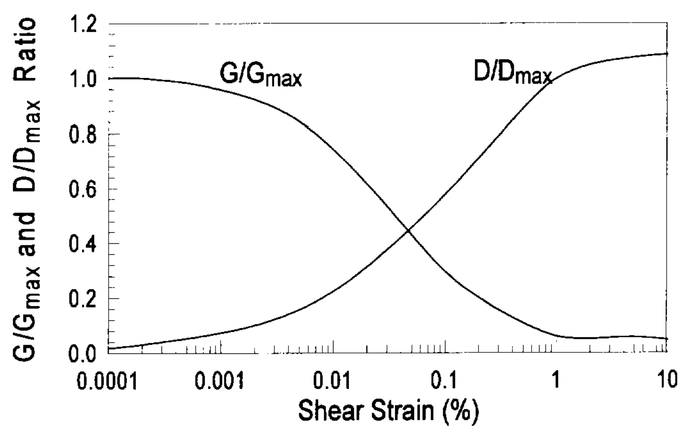

Fig. 17. Variation of shear modulus and damping ratio of sand with shear strain [Seed and Idriss, 1970].

PILE-3D analyzes the soil in terms of total stresses. The program has been modified for effective stress analysis by including a porewater pressure model for the generation of seismic porewater pressures due to shaking. The modified program is designated PILE-3DF. The porewater pressure model used is that developed by Martin, Finn and Seed [1975] but modified by adopting the two parameter model for volume change suggested by Byrne [1991]. During seismic response analysis, the soil properties are changed continuously to reflect the effects of the seismic porewater pressures on moduli and strength.

The effective stress analysis program PILE-3DF was validated using data from centrifuge tests on single piles and pile groups in liquefiable soils. These tests were run at the University of California at Davis and have been reported by Wilson et al. [1995] and Wilson et al. [1997]. The centrifuge tests and the validation process are described in the following two sections.

CENTRIFUGE TESTS

Dynamic centrifuge tests of pile supported structures in liquefiable sand were performed on the large centrifuge at University of California at Davis, California. The models consisted of two structures supported by single piles, one structure supported by a 2×2 pile group and one structure supported by a 3×3 pile group. The typical arrangement of structures and instrumentation is shown in Fig. 18. Full details of the centrifuge tests can be found in Wilson et al. [1997]. Only the single pile system (SP1) and the (2×2) pile group (GP1) are discussed here.

The model dimensions and the arrangement of strain gauges in systems SP1 and GP1 are shown in Figs. 19 and 20, respectively. Model tests were performed at a centrifugal acceleration of 30g.

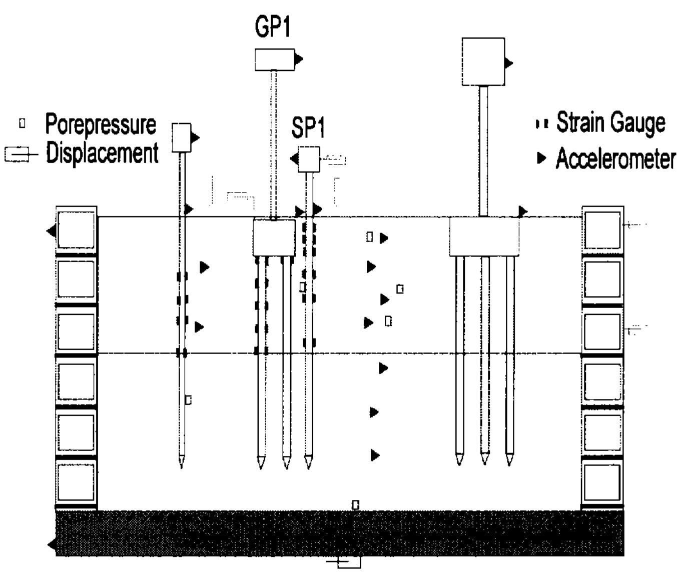

Fig. 18. Layout of models for centrifuge tests.

The soil profile consists of two level layers of Nevada sand, each approximately 10m thick at prototype scale. Nevada sand is a uniformly graded fine sand with a coefficient of uniformity of 1.5 and mean grain size of 0.15 mm. Sand was air pluviated to relative densities of 75%-80% in the lower layer and 55% in the upper layer. Prior to saturation, any entrapped air was carefully removed. The container was then filled with a hydroxy-propyl methyl-cellulose and water mixture under vacuum. The viscosity of this pore fluid is about ten times greater than pure water to ensure proper scaling. Saturation was confirmed by measuring the compressive wave velocity from the top to the bottom of the soil profile.

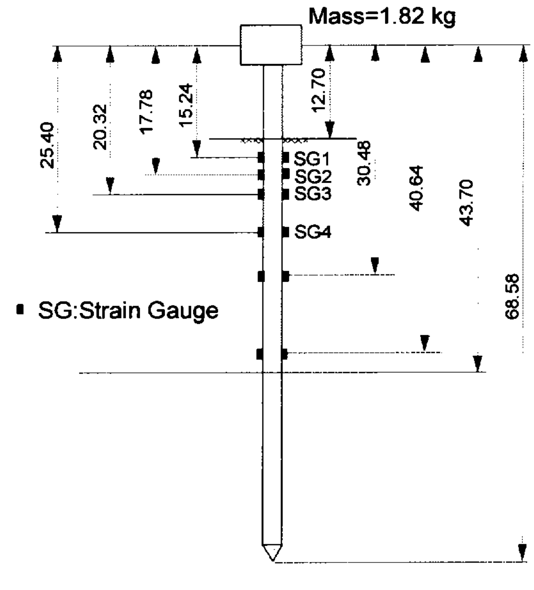

Fig. 19. Instrumented pile for single pile test.

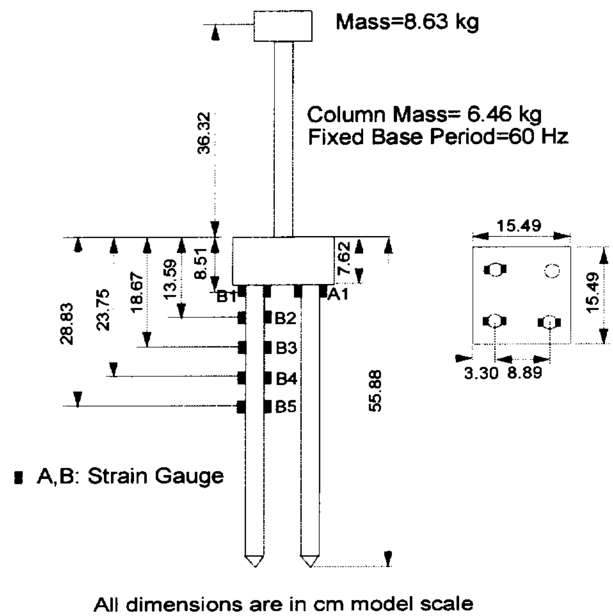

Fig. 20. Instrumented test piles and superstructure.

The responses of the single pile and the 2×2 pile group to the Santa Cruz acceleration record obtained during the 1989 Loma Prieta earthquake, scaled to 0.49 g is described and analyzed here. For some additional details see Finn et al [1999].

EFFECTIVE STRESS DYNAMIC ANALYSIS OF PILES-SUPERSTRUCTURE

The finite element mesh used in the analysis is shown in Fig. 21. The finite element model consists of 1649 nodes and 1200 soil elements. The upper sand layer which is 9.1 m thick was divided into 11 layers and the lower sand layer which is 11.4 m thick was divided into 9 layers. The single pile was modeled with 28 beam elements. 17 beam elements were within the soil strata and 11 elements were used to model the free standing length of the pile above the soil. The superstructure mass was treated as a rigid body and its motion is represented by a concentrated mass at the center of gravity. A rigid beam element was used to connect the superstructure to the pile head.

Soil and Pile Properties

The small strain shear moduli G_{max}, were estimated using the formula proposed by Seed and Idriss [1970].

$$G_{max} = 21.7\, k_{max}\, P_a \left(\sigma'_m / P_a\right)^{0.5} \tag{3}$$

in which k_{max} is a constant which depends on the relative density of the soil, σ'_m is the initial mean effective stress and P_a is the atmospheric pressure. The program PILE-3DF accounts for the changes in shear moduli and damping ratios due to dynamic shear strains at the end of each time increment. The shear strain dependencies of the shear modulus and damping ratio of the soil were defined by the curves suggested by Seed and Idriss [1970] for sand. The friction angles of the upper and the lower layers were taken as 35° and 40°, respectively.

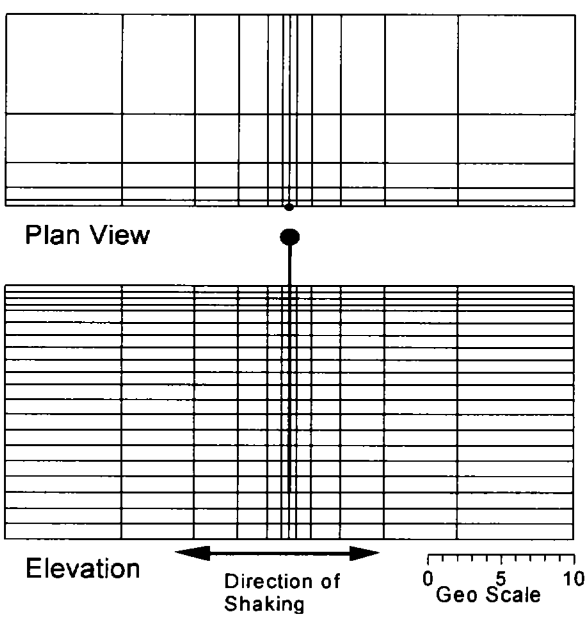

Fig. 21. Finite element mesh for single pile.

Porewater Pressure Effects

Increments in seismic porewater pressures were generated in each individual element depending on the accumulated volumetric strain prevailing in that element and the current increment in volumetric strain. The moduli and shear strengths of the foundation soils were modified continuously to account for the effects of the changing seismic porewater pressures.

Earthquake Input Motion

The Santa Cruz acceleration record from the 1989 Loma Prieta earthquake was scaled to 0.49 g and used as input to the shake table. The base accelerations of the model were measured at the east and west ends of the base of the model container. Wilson et al.[1995] showed that both accelerations agreed very well.
The base input acceleration is shown in Fig. 22.

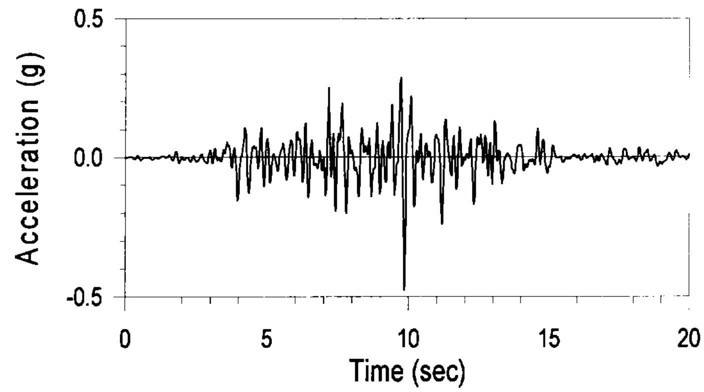

Fig. 22. Input acceleration time history.

Results of Single Pile Analysis

Acceleration Response: Figure 23 shows the measured and computed acceleration response of the superstructure. There is generally good agreement between them, especially in the time period of peak response.

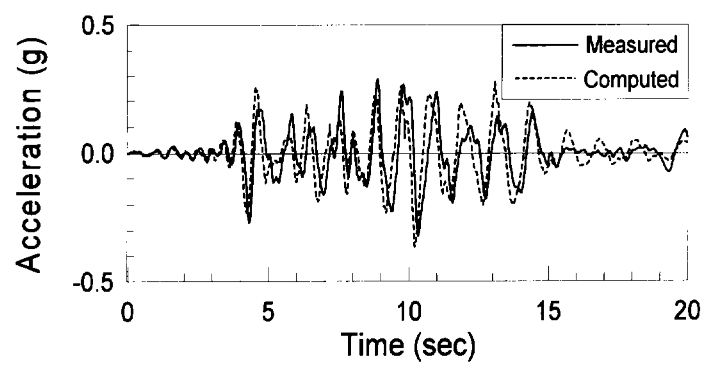

Fig. 23. Comparison of measured and computed superstructure acceleration time histories.

Porewater Pressure Response: Figure 24 shows comparisons between measured and computed porewater pressures at three different depths; 1.14 m, 4.56 m, and 6.78 m in the free field. The agreement is very good.

Bending Moment Response: Figure 25 shows the measured and computed bending moment time histories at two different depths; 0.76 m and 1.52 m. Generally there is a very good agreement between the measured and computed time histories.

Figure 26 shows the profiles of measured and computed maximum bending moments with depth. The comparison between measured and computed moments is fairly good, although the maximum moment is overestimated by 10%-20% between 1 m and 4 m depths.

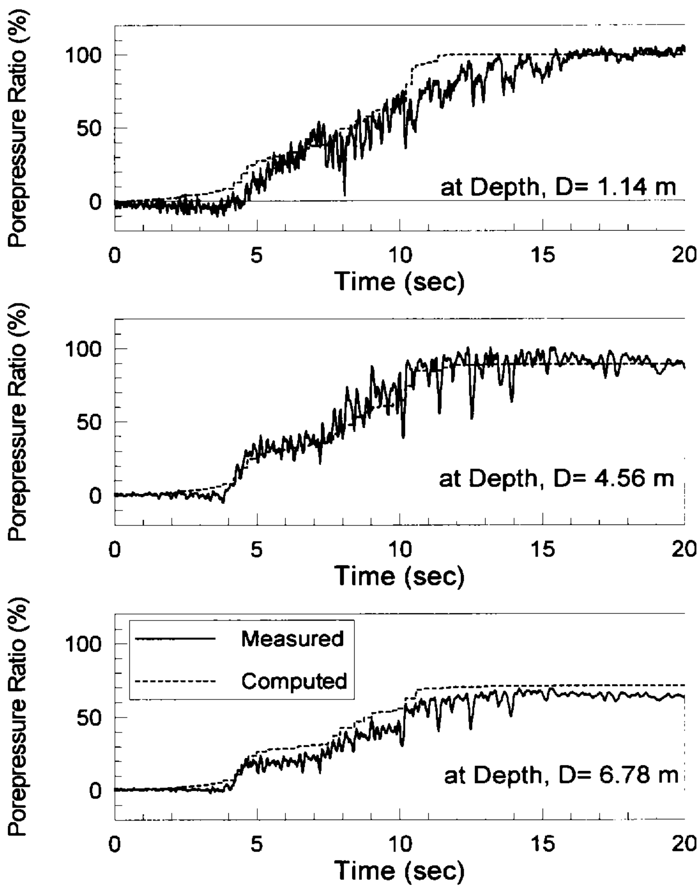

Fig. 24. Comparison of measured and computed porewater pressure time histories at three depths.

Analysis of 2×2 Pile Group

Effective stress analyses were also carried out to simulate the response of the (2×2) pile group- superstructure system. The finite element mesh is similar in type to that in Fig. 22 except for the presence of the pile cap.
The pile cap was modeled with 16 brick elements and treated as rigid body. The superstructure mass was treated as a rigid body and its motion was represented by a concentrated mass at the center of gravity. The column carrying the superstructure mass was modeled using beam elements and is treated as a linear elastic structure. As the stiffness of this column element was not reported, it was calculated based on the fixed base frequency of the superstructure given as 2 Hz by Wilson et al. [1997].

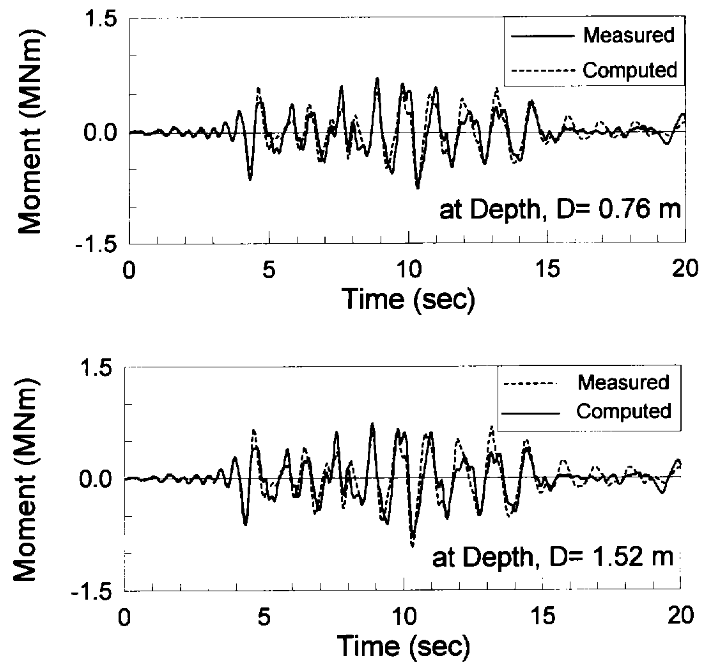

Fig. 25. Comparison of measured and computed bending moment time histories at two depths.

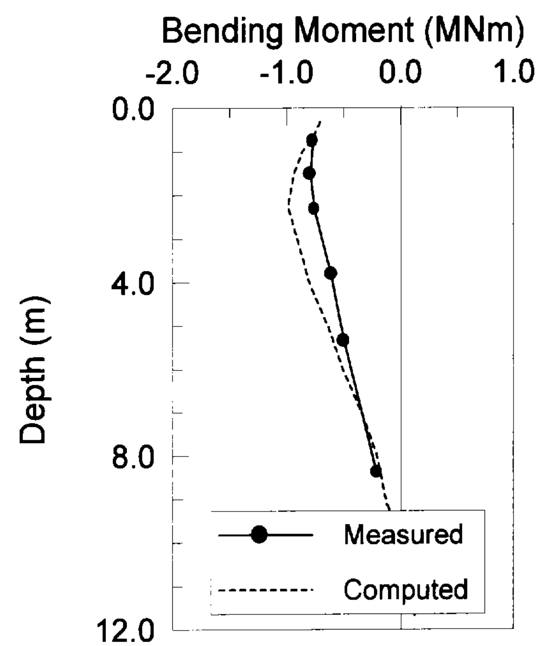

Fig. 26. Comparison of measured and computed maximum bending moments profiles along the pile.

Results of (2×2) Group Pile Analysis

Acceleration Response: Figure 27 shows computed and measured pile cap acceleration time histories. There is a good agreement between the measured and computed values.

Bending Moment Response: Figure 28 shows time histories of measured and computed moments at a depth of 2.55 m. The measured and computed time histories compare quite well. Residual moments were removed from the time history of measured moments before the comparison was made.

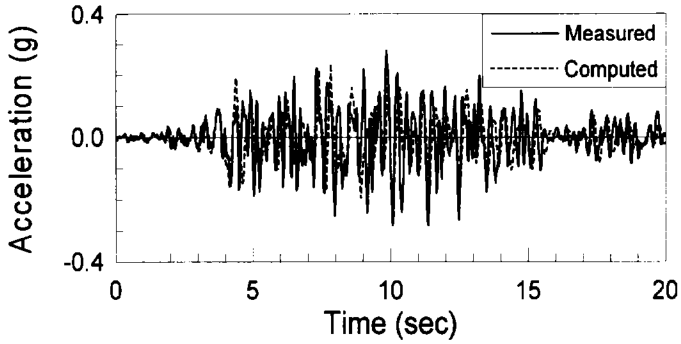

Fig. 27. Comparison of measured and computed pile cap acceleration time histories.

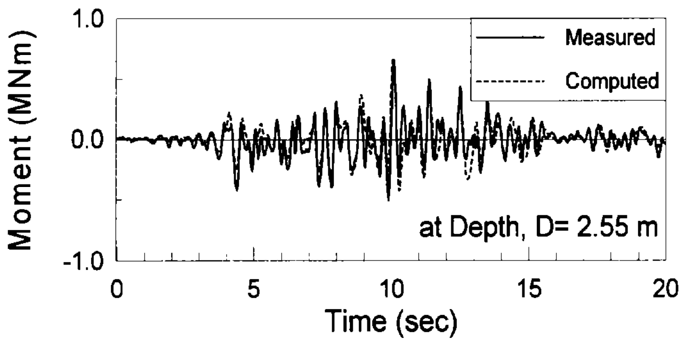

Fig. 28. Comparison of measured and computed bending moment time histories.

Figure 29 shows the measured and computed bending moment profiles with depth. They also compare very well.

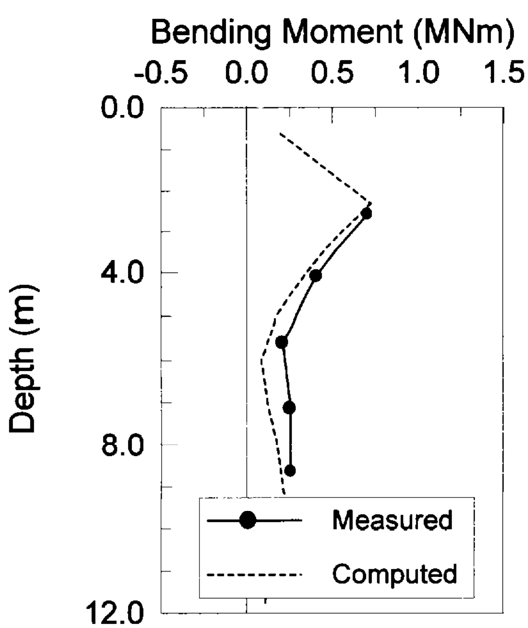

Fig. 29. Comparison of measured and computed maximum bending moments along the pile.

CONCLUSIONS

Several case histories showing severe damage to pile foundations in liquefied soils are presented. All these cases involve piles which were designed to carry vertical loads only. They were installed to control settlements or to carry building loads to competent soil layers. Often these piles are concrete pipe piles with only nominal reinforcement. During an earthquake these piles are first subjected dynamic lateral forces and moments and then are loaded by lateral spreading of liquefied soils. Frequently the failure is attributed to effects of lateral spreading only. In the case of the 1995 Kobe earthquake in which very high ground accelerations were experienced, many of the failed piles must have sustained at least extensive cracking before significant lateral spreading occurred. Such damage is rarely taken into account when analysing the effects of lateral spreading. The dramatic damage to these weak piles gives a distorted picture of the capacity of piles to resist lateral ground displacement. Piles can be designed economically to perform well in liquefied ground. Example were presented in which piles were undamaged despite lateral displacements up to 2 m.

A dynamic effective stress analysis, followed by an analysis of lateral spreading effects are necessary to understand fully the failure mechanisms and to predict field performance. The analysis of the collapse of a deck section of the Nishinomiya Bridge during the 1995 Kobe earthquake illustrates the importance of a comprehensive analysis of the structure-foundation-soil system in order to understand potential or actual seismic performance of pile foundations in liquefied soils.

In engineering practice, the seismic response of pile foundations is modeled by analysis a single pile and pile group response is developed from single pile response using elastic interaction factors or empirical group factors. For the single pile analysis, the interaction between soil and pile is modeled by nonlinear springs (p-y curves) and dashpots. Even under static loading, as noted in the text, this type of analysis seems to be rather unreliable on the basis of field loading test data. Seismic analysis of piles in centrifuge test shows similar unreliability.

The nonlinear quasi-3D program, PILE-3DF, has been presented for dynamic effective stress analysis of piles and pile groups in liquefiable soils. This program was validated using data from centrifuge tests on single piles and pile groups in liquefied soils conducted at the University of California, Davis, California. PILE-3DF could simulate the recorded response of these pile foundations with an accuracy sufficient for engineering purposes.

There is considerable uncertainty surrounding all methods of post-liquefaction displacements analysis. The simplest type of analysis is a force based analysis such as that recommended by the Japan Water Works Association (JWWA). In the JWWA analysis the liquefied soils are assumed to apply pressures not exceeding 30 % of the total overburden pressure to the piles. Any unliquefied layers riding on the liquefied soil are assumed to apply passive pressures.

Another approach is to use the soil-pile model described above and apply the estimated ground displacements to the end of the near field springs. In the absence of site specific load test data to define linear or nonlinear spring properties, this approach has been shown to be somewhat unreliable.

ACKNOWLEDGMENTS

This work was supported financially by the National Science and Engineering Council of Canada under Grant No. 1498 and by Anabuki Komuten, Takamatsu, Japan. The invaluable assistance of Noboru Fujita in the preparation of the paper is gratefully acknowledged.

REFERENCES

Abghari, A. and J. Chai, [1995]. Modeling of soil-pile-superstructure interaction for bridge foundations. Performance of Deep Foundations Under Seismic Loading, ASCE Geot. Special Publ. No. 51, pp. 45-59.

API [1993]. Recommended practice for planning, designing, and constructing fixed offshore platforms. American Petroleum Institute, Washington, D.C.

Byrne, P.M. [1991]. A cyclic shear-volume coupling and pore pressure model for sand. Proc. 2nd Int. Conf. on Recent Advances in Geotechnical Earthquake Eng. and Soil Dynamics, St. Louis, Report 1.24, 1:47-56.

Finn, W.D. Liam and W.B. Gohl, [1987]. Centrifuge model studies of piles under simulated earthquake loading from dynamic response of pile foundations - experiment, analysis and observation. ASCE Convention, Atlantic City, New Jersey, Geotechnical Special Publication No. 11, pp. 21-38.

Finn, W.D. Liam and G. Wu, [1994]. Recent developments in dynamic analysis of piles. Proc., 9th Japan Conference on Earthquake Engineering, Tokyo, Japan, Vol. 3, pp. 325-330.

Finn W. D. Liam, T. Thavaraj, D.W. Wilson, R.W. Boulanger, and K. Kutter, [1999]. Seismic analysis of piles and pile groups in liquefiable sands, Proceedings, 7th International Symposium on Numerical Models in Geomachanics – NUMOG VII, Graz, Austria, September, A. A. Balkema, Rotterdam/Brookfield, pp-287-292.

Gazetas, G. and R. Dobry, [1984]. Horizontal response of piles in layered soils. J. of Geotech. Eng., Vol. 110, No. 1, Jan., pp. 20-40.

Gazetas, G., K. Fan, and A. Kaynia, [1993]. Dynamic response of pile groups with different configurations. Soil Dynamics and Earthquake Engineering, 12:239-257.

Gazioglu, S.M. and M.W. O'Neill, [1984]. An evaluation of the p-y relationships in cohesive soils. Proc. of the ASCE Symposium on Analysis and Design of Pile Foundations, ASCE National Convention, San Francisco, California, Oct. 1-5, 1984, Edited by J.R. Meyer, pp. 192-213.

Hamada, M., S. Yasuda, R. Isoyama and K. Emoto, [1986] Study on liquefaction induced permanent ground displacements, Report for the Association for the Development of Earthquake Prediction.

Martin, G.R., W.D. Liam Finn, and H.B. Seed, [1975]. Fundamentals of liquefaction under cyclic loading. Journal of Geotechnical Engineering Division. ASCE, Vol. 101, GT5:423- 438.

Murchison, J.M. and M.W. O'Neill, [1984], An evaluation of p-y relationships in cohesionless soils. Proc. of the ASCE Symposium on Analysis and Design of Pile Foundations, ASCE National Convention, San Francisco, California, Oct 1-5, 1984, Edited by J. R. Meyer, pp. 174-191.

Novak, M. [1991]. Piles under dynamic loads. State of the Art Paper, 2nd International Conference Recent Advances in Geotechnical Earthquake Engineering and Soil Dynamics, University of Missouri-Rolla, Rolla, Missouri, Vol. III, pp. 250-273.

Seed, H.B. and I.M. Idriss, [1970]. Soil moduli and damping factors for dynamic response analysis. Report #EERC70-10, Earthquake Engineering Research Center, Berkeley, CA.

Wilson, D.W., R.W. Boulanger, and B.L. Kutter, [1997]. Soil-pile-superstructure interaction at soft or liquefiable sites - Centrifuge data report for CSP1-5. Report No. UCD/CGMDR-97/01-05, Center for Geotechnical Modeling, Dept. of Civil and Environmental Eng., University of California at Davis, CA.

Wilson, D.W., R.W. Boulanger, and B.L. Kutter, and A. Abghari, [1995]. Dynamic centrifuge tests of pile supported structures in liquefiable sand. Proc., National Seismic Conf. on Bridges and Highways. Sponsored by Federal Highways Admin. and CALTRANS, San Diego, CA.

Wu, G. and W.D. Liam Finn, [1994]. PILE-3D - prototype program for nonlinear dynamic analysis of pile groups. Dept. of Civil Engineering, University of B.C., Vancouver.

Wu, G. and W.D. Liam Finn, [1997a]. Dynamic elastic analysis of pile foundations using finite element method in the frequency domain. Canadian Geotechnical J., Vol. 34, 1:34-43.

Wu, G. and W.D. Liam Finn, [1997b]. Dynamic nonlinear analysis of pile foundations using finite element method in the time domain. Canadian Geotechnical J., Vol. 34, 1:44-52.